

Article

Risk of Crop Yield Reduction in China under 1.5 °C and 2 °C Global Warming from CMIP6 Models

Feiyu Wang ¹, Chesheng Zhan ² and Lei Zou ^{1,*}

¹ Key Laboratory of Water Cycle and Related Land Surface Processes, Institute of Geographic Sciences and Natural Resources Research, Chinese Academy of Sciences, Beijing 100101, China

² Key Laboratory of Ecosystem Network Observation and Modeling, Institute of Geographic Sciences and Natural Resources Research, Chinese Academy of Sciences, Beijing 100101, China

* Correspondence: zoulei@igsnr.ac.cn

Abstract: Warmer temperatures significantly influence crop yields, which are a critical determinant of food supply and human well-being. In this study, a probabilistic approach based on bivariate copula models was used to investigate the dependence (described by joint distribution) between crop yield and growing season temperature (T_{GS}) in the major producing provinces of China for three staple crops (i.e., rice, wheat, and maize). Based on the outputs of 12 models from the Coupled Model Intercomparison Project Phase 6 (CMIP6) under Shared Socioeconomic Pathway 5–8.5, the probability of yield reduction under 1.5 °C and 2 °C global warming was estimated, which has great implications for agricultural risk management. Results showed that yield response to T_{GS} varied with crop and region, with the most vulnerable being rice in Sichuan, wheat in Sichuan and Gansu, and maize in Shandong, Liaoning, Jilin, Nei Mongol, Shanxi, and Hebei. Among the selected five copulas, Archimedean/elliptical copulas were more suitable to describe the joint distribution between T_{GS} and yield in most rice-/maize-producing provinces. The probability of yield reduction was greater in vulnerable provinces than in non-vulnerable provinces, with maize facing a higher risk of warming-driven yield loss than rice and wheat. Compared to the 1.5 °C global warming, an additional 0.5 °C warming would increase the yield loss risk in vulnerable provinces by 2–17%, 1–16%, and 3–17% for rice, wheat, and maize, respectively. The copula-based model proved to be an effective tool to provide probabilistic estimates of yield reduction due to warming and can be applied to other crops and regions. The results of this study demonstrated the importance of keeping global warming within 1.5 °C to mitigate the yield loss risk and optimize agricultural decision-making in vulnerable regions.

Keywords: global warming; crop yield; risk; China



Citation: Wang, F.; Zhan, C.; Zou, L. Risk of Crop Yield Reduction in China under 1.5 °C and 2 °C Global Warming from CMIP6 Models. *Foods* **2023**, *12*, 413. <https://doi.org/10.3390/foods12020413>

Academic Editors: Bojan Šarkanj, Ines Sviličić Petrić and Dunja Šamec

Received: 16 November 2022

Revised: 13 December 2022

Accepted: 13 January 2023

Published: 15 January 2023



Copyright: © 2023 by the authors. Licensee MDPI, Basel, Switzerland. This article is an open access article distributed under the terms and conditions of the Creative Commons Attribution (CC BY) license (<https://creativecommons.org/licenses/by/4.0/>).

1. Introduction

The global surface temperature during the first two decades of the 21st century (2001–2020) has increased by 0.99 °C compared to the pre-industrial level (1850–1900), with a larger increase on land than in the ocean [1]. This warming trend is projected to continue in the following decades with rising greenhouse gas emissions, particularly in cultivated areas [2–5]. Given that global food demand is expected to double by the 2050s [3,6,7], global warming will pose more challenges to crop yield and food supplies for the next several decades. Therefore, it is crucial to estimate the possible changes in crop yield within the context of global warming.

Previous studies have shown that crop yields are affected by numerous climatic factors (e.g., temperature, precipitation, and drought) and their interactions [2,8–13]. Among these factors, temperature changes (i.e., warming trends) are expected to be more deterministic than others [14], and thus estimating temperature effects on crop yields is essential for climate change risk management. Generally, in most regions, higher temperatures can

reduce crop yields by accelerating crop growth and shortening the growing period, or by exacerbating the negative impact of other factors on yield, such as warming-driven drought and compound dry-hot events [8,15–18]. However, warming may positively affect crop yields in other areas, such as those with heat deficits and those with adaptive measures (e.g., alteration of cultivar, planting dates, and irrigation types) [5,17,19–21]. Hence, the different mechanisms of temperature effects on crop growth lead to uncertainty in estimating possible yield changes under global warming.

Many approaches have been employed to study the climatic effect on crop yield, including field experiments, statistical regression, and crop model simulations [5,14,22–25]. For instance, Zhao et al. [14] investigated the temperature impact on yields of four crops (wheat, rice, maize, and soybean) based on four analytical methods and the authors found that temperature negatively affected yield at the global scale. Ray et al. [25] used a statistical crop time series for ~13,500 political units to analyze the variations in yields of maize, rice, wheat, and soybean caused by climate change and indicated that climate variability accounted for roughly one-third (~32–39%) of the observed yield variability. However, most previous studies have provided deterministic rather than probabilistic estimates of temperature effects on crop yield [26–28]. In practice, it is difficult to obtain an accurate estimate due to inevitable uncertainties in model structure or parameters, data quality, and incomplete consideration of the physical mechanisms related to crop growth [2,8,12,14,29]. In this case, the probability-based approach helps better characterize the yield-temperature relationship and its variation under warming conditions [30–32]. Among probabilistic models, copula-based models have been widely used in agriculture to explore the dependence between crop yields and climate variability (e.g., precipitation, soil moisture, solar radiation, and temperature) [11,23]. Based on the joint probability distribution of two individual variables (e.g., yield and temperature), the copula functions enable flexible estimation of the conditional probability of one variable when a certain threshold is exceeded for the other variable [33].

A new global temperature goal was recently established in the Paris Agreement to limit the increase in global temperature to 2 °C above pre-industrial levels, and preferably to 1.5 °C [34]. This goal aims to minimize the risk of climate change worldwide. Herein, we focused on the risk of yield reduction under 1.5 °C and 2 °C global warming, i.e., the probability of yield reduction in response to higher temperatures. Meanwhile, China is the second largest crop-producing country in the world, contributing to 17.4%, 21.9%, and 14.8% of the total global production of maize, rice, and wheat, respectively [12]. This indicates that crop yield in China is a matter of both domestic and global food supplies, especially given the threat of global warming and the continuously increasing population [27,35].

In this study, a copula-based approach is developed to model the joint probability distribution of crop yield and temperature for assessing the possible outcomes of yield changes under 1.5 °C and 2 °C global warming scenarios. This study was conducted on the main producing provinces corresponding to three staple crops (i.e., rice, wheat, and maize) in China, focusing on those provinces vulnerable to warming. The objectives of this study were to: (1) investigate the dependence between crop yield and temperature; (2) examine the yield sensitivity to different temperature conditions; and (3) estimate the risk of yield loss at 1.5 °C and 2 °C global warming targets.

2. Materials and Methods

2.1. Crop Yield and Meteorological Data

We obtained annual crop yield data (from 1995 to 2014) and crop production data (from 2015 to 2019) for rice, wheat, and maize for all provinces (or autonomous regions) from the China Agriculture Statistical Report, compiled by the Ministry of Agriculture and Rural Affairs of the People's Republic of China. The top ten producing provinces for each crop were selected as the study area based on the average crop production in recent years (2015–2019). For each crop, the sum of production in the top ten producing provinces accounted for more than 80% of the total national production. The growing season and cropping system information for each crop-province pair were collected from previous

studies and the agricultural atlas [36–43], as shown in Table 1. The long-term average annual yield and growing season temperature during the reference period are also shown in Table 1.

Table 1. Crop-producing information for each crop-province pair.

| Type | Province | Short Name | Growing Season | Cropping System |
|-------|--------------|------------|----------------|-----------------|
| Rice | Heilongjiang | HLJ | May-September | Single rice |
| | Jiangsu | JS | April-October | Single rice |
| | Zhejiang | ZJ | April-November | Double rice |
| | Anhui | AH | April-November | Double rice |
| | Jiangxi | JX | April-November | Double rice |
| | Hubei | HB | April-November | Double rice |
| | Hunan | HN | April-November | Double rice |
| | Guangdong | GD | March-November | Double rice |
| | Guangxi | GX | March-November | Double rice |
| | Sichuan | SC | April-October | Single rice |
| Wheat | Hebei | HB2 | October-May | Winter wheat |
| | Jiangsu | JS | November-May | Winter wheat |
| | Anhui | AH | November-April | Winter wheat |
| | Shandong | SD | September-June | Winter wheat |
| | Henan | HN2 | September-June | Winter wheat |
| | Hubei | HB | November-April | Winter wheat |
| | Sichuan | SC | November-May | Winter wheat |
| | Shaanxi | SX | October-June | Winter wheat |
| | Gansu | GS | October-June | Winter wheat |
| | Xinjiang | XJ | October-June | Winter wheat |
| Maize | Hebei | HB2 | June-September | Summer maize |
| | Shanxi | SX2 | May-September | Spring maize |
| | Nei Mongol | NM | May-September | Spring maize |
| | Liaoning | LN | May-September | Spring maize |
| | Jilin | JL | May-September | Spring maize |
| | Heilongjiang | HLJ | May-September | Spring maize |
| | Shandong | SD | June-September | Spring maize |
| | Henan | HN2 | June-September | Spring maize |
| | Sichuan | SC | June-September | Summer maize |
| | Yunnan | YN | June-September | Summer maize |

The observational temperature dataset during 1994–2014 was derived from a daily high-resolution ($0.5^\circ \times 0.5^\circ$) meteorological dataset (i.e., CN05.1) [44] provided by the National Climate Center of the China Meteorological Administration. It should be noted that temperature data were collected from 1994 (one year ahead of crop yield data) because the growing season for winter wheat starts from the previous winter. This dataset was constructed based on interpolation from over 2416 station observations across China and has been widely used to evaluate climate model performance and analyze the climate characteristics of China [45–47]. It has proven to be a reliable reproduction of the historical climate in China [48,49]. The monthly temperatures were then calculated based on the daily data derived from the arithmetic mean. In addition, the simulated daily temperature data for the historical period and future scenario experiment were derived from 12 models of Coupled Model Inter-comparison Project Phase 6 (CMIP6), as listed in Table 2. This study focused on the high-emission shared socioeconomic pathway 5-8.5 (SSP5-8.5). All the model projections were bias-corrected and downscaled using the Bias Correction and Spatial Downscaling approach (BCSD), which has been widely used in the meteorological field [50–52].

The spatially weighted average temperature for each province was calculated based on the weight defined by the crop harvested area mapping in 2000, acquired from the data center of the global spatial production allocation model (SPAM) (<http://mapspam.info/data/>, accessed on 11 August 2022) (Figure 1). According to the growing season information (Table 1), the annual growing season temperature (T_{GS}) was calculated from the average

monthly temperatures during the growing season. The first-difference method was used to detrend the yield and T_{GS} data to eliminate the confounding influence of long-term variations, such as changes in crop management and technological advancement [9,53,54].

Table 2. Information of 12 CMIP6 models used in this study.

| Model | Country | Modeling Center | Resolution (lat × lon) |
|-----------------|-----------|--|------------------------|
| ACCESS-ESM1-5 | Australia | Commonwealth Scientific and Industrial Research Organization and Bureau of Meteorology | 1.25° × 1.875° |
| BCC-CSM2-MR | China | Beijing Climate Center | 1.125° × 1.125° |
| EC-Earth3 | Europe | EC-EARTH consortium | 0.7° × 0.7° |
| FGOALS-g3 | China | State Key Laboratory of Numerical Modeling for Atmospheric Sciences and Geophysical Fluid Dynamics (LASG), Institute of Atmospheric Physics, Chinese Academy of Sciences | 2.25° × 2° |
| GFDL-CM4 | USA | NOAA Geophysical Fluid Dynamics Laboratory | 1.0° × 1.25° |
| GFDL-ESM4 | USA | NOAA Geophysical Fluid Dynamics Laboratory | 1.0° × 1.25° |
| HadGEM3-GC31-LL | UK | Met Office Hadley Centre | 1.25° × 1.875° |
| INM-CM4-8 | Russia | Institute for Numerical Mathematics, Russian Academy of Science | 1.5° × 2° |
| MIROC6 | Japan | National Institute for Environmental Studies, University of Tokyo | 1.4° × 1.4° |
| MIROC-ES2L | Japan | National Institute for Environmental Studies, University of Tokyo | 2.8° × 2.8° |
| MPI-ESM1-2-LR | Germany | Max Planck Institute for Meteorology | 1.875° × 1.875° |
| MRI-ESM2-0 | Japan | Meteorological Research Institute | 1.125° × 1.125° |

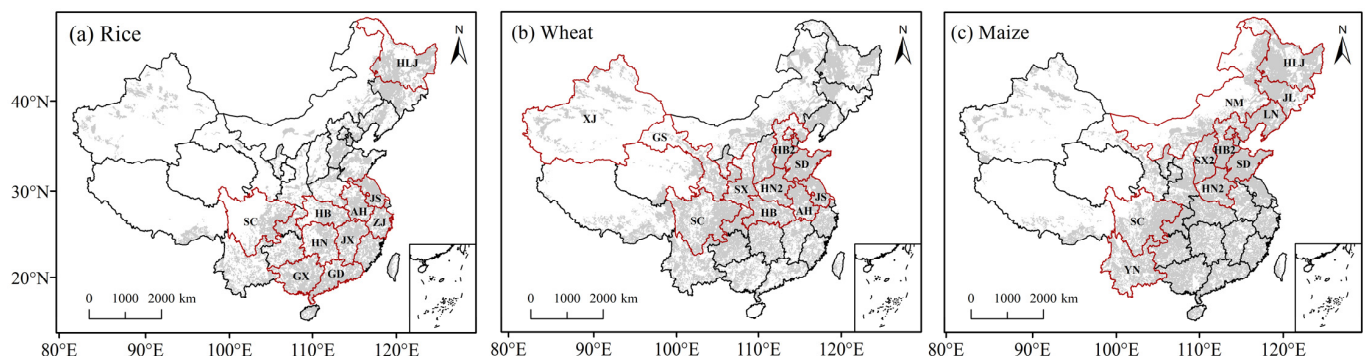


Figure 1. Main crop-producing provinces for (a) rice, (b) wheat, and (c) maize, respectively. The grey-shaded areas indicate the harvested areas. The provinces surrounded by red lines represent the top 10 producing provinces. The full names of the abbreviations for each province can be found in Table 1.

2.2. Copula-Based Model

Copula functions are powerful tools to describe the dependence structure between random variables [33,55]. In this study, we used the bivariate copula model to construct the joint probability distribution of temperature (X) and crop yield (Y) based on their univariate distributions. According to Sklar's theorem [56], a joint cumulative distribution function (CDF) can be expressed as follows:

$$F_{X,Y}(x,y) = C[u,v] \quad (1)$$

where u and v denote the marginal distribution functions of X and Y , which are uniformly distributed in the domain of 0 to 1 [33], and copula C describes the bivariate joint CDF of u and v .

The most commonly used copula families in meteorological and hydrological studies are elliptical and Archimedean copulas [11,23,57]. Herein, two popular elliptical copulas (i.e., Gaussian and t) and three Archimedean copulas (i.e., Frank, Clayton, and Gumbel) were chosen to model the joint probability distribution between temperature (X) and yield (Y), as listed in Table 3. Different copulas reflect different characteristics of the overall de-

pendence structure and the tail dependence, with the latter describes the joint distribution between the extreme values of the variables, which is important for risk analysis. Among these five copulas, the Gaussian, t, and Frank copulas describe symmetric dependence structures, i.e., the same degree of dependence in the upper and lower tails (which correspond to extreme values), but with different behaviors at the corners of quadrants. In contrast, the Clayton and Gumbel copulas characterize an asymmetric tail dependence with a greater dependence in the lower and upper tails, respectively.

Table 3. Summary of five commonly used bivariate copulas.

| Name | Function | Parameter Range |
|----------|--|-------------------------------------|
| Gaussian | $C(u, v) = \int_{-\infty}^{\Phi^{-1}(u)} \int_{-\infty}^{\Phi^{-1}(v)} \frac{1}{2\pi\sqrt{1-\theta^2}} \exp\left\{-\frac{x^2+y^2-2\theta xy}{2(1-\theta^2)}\right\} dx dy$ | $\theta \in (-1, 1)$ |
| t | $C(u, v) = \int_{-\infty}^{t_v^{-1}(u)} \int_{-\infty}^{t_v^{-1}(v)} \frac{1}{2\pi\sqrt{1-\theta^2}} \exp\left\{1 + \frac{x^2+y^2-2\theta xy}{v(1-\theta^2)}\right\}^{-\frac{v+2}{2}} dx dy$ | $\theta \in (-1, 1)$ |
| Clayton | $C(u, v) = (u^{-\theta} + v^{-\theta} - 1)^{-1/\theta}$ | $\theta \in [0, \infty)$ |
| Frank | $C(u, v) = -\frac{1}{\theta} \ln \left[1 + \frac{(e^{-\theta u} - 1)(e^{-\theta v} - 1)}{e^{-\theta} - 1} \right]$ | $\theta \in \mathbb{R} \setminus 0$ |
| Gumbel | $C(u, v) = \exp\left\{-\left[(-\ln u)^\theta + (-\ln v)^\theta\right]^{\frac{1}{\theta}}\right\}$ | $\theta \in [1, +\infty)$ |

Based on the joint distribution between X and Y, the conditional probability of Y dropping below a certain threshold ($Y < y$) under different X conditions ($X = x_1, x_2, \dots$), i.e., $P(Y < y \mid X = x)$, can be estimated. The conditional probability density function (PDF) can be expressed as follows [32,58]:

$$f_{Y|X}(y|x) = c[u, v] \cdot f_Y(y) \tag{2}$$

where c denotes the joint PDF of the copula function, and $f_Y(y)$ denotes the PDF of the marginal distribution for Y. Once the conditional PDF is determined, the probability $P(Y < y \mid X = x)$ can be calculated as the area under the PDF curve within the interval $(-\infty, y]$. Obviously, the area under the whole PDF curve is always exactly 1.

The data processing flow is as follows. First, the marginal distributions were fitted to the detrended yield (ΔYield) and T_{GS} (ΔT_{GS}). Second, the five bivariate copulas were fitted to ΔYield and ΔT_{GS} data, and the optimal copula was selected based on the comprehensive goodness of fit measures, including the Akaike information criterion (AIC), Bayesian information criterion (BIC), root mean square error (RMSE), and Nash-Sutcliffe efficiency (NSE) [59]. The conditional PDFs for different ΔT_{GS} conditions were then determined. Finally, the probability of yield reduction (i.e., $\Delta\text{Yield} < 0$) for each warming condition (i.e., 1.5 °C and 2 °C global warming) was estimated. All data processing and analysis work was implemented based on the MATLAB platform.

2.3. Dependence Measure

Spearman’s rank correlation coefficient (ρ) is a measure that assesses the extent to which a monotonic function can describe the dependence between two random variables, X and Y. Since it is defined by the rank of given data rather than the data itself, it remains scale-invariant under strictly increasing transformations of the random variables [33]. Hence, when working with copulas, Spearman’s ρ is more appropriate than Pearson’s correlation coefficient (which measures the linear dependence between random variables). The Spearman’s ρ (ρ_S) for random variables X and Y can be expressed by the copula $C(u, v)$ as follows [33]:

$$\rho_S = 12 \iint_{[0,1]^2} uv dC(u, v) - 3 \tag{3}$$

where u and v denote the marginal distribution functions of X and Y , as mentioned earlier.

2.4. Timing of Reaching the Global Warming Targets

The global warming targets of 1.5 °C and 2 °C refer to global mean surface temperature (GMST) increases of 1.5 °C and 2 °C above the pre-industrial level. Since the reference period was defined as 1995–2014 in this study, a 20-year time window was used to determine the timing of reaching the 1.5 °C and 2 °C global warming targets. The specific timing of reaching the global warming targets was then determined as the first time window when the GMST of each climate model reached 1.5 °C and 2 °C above the pre-industrial equivalent. As shown in Figure 2, this timing under SSP5-8.5 varied with the climate model. Thus, we used a multi-model ensemble mean to reduce the uncertainty caused by differences among models to analyze the yield response to future warming.

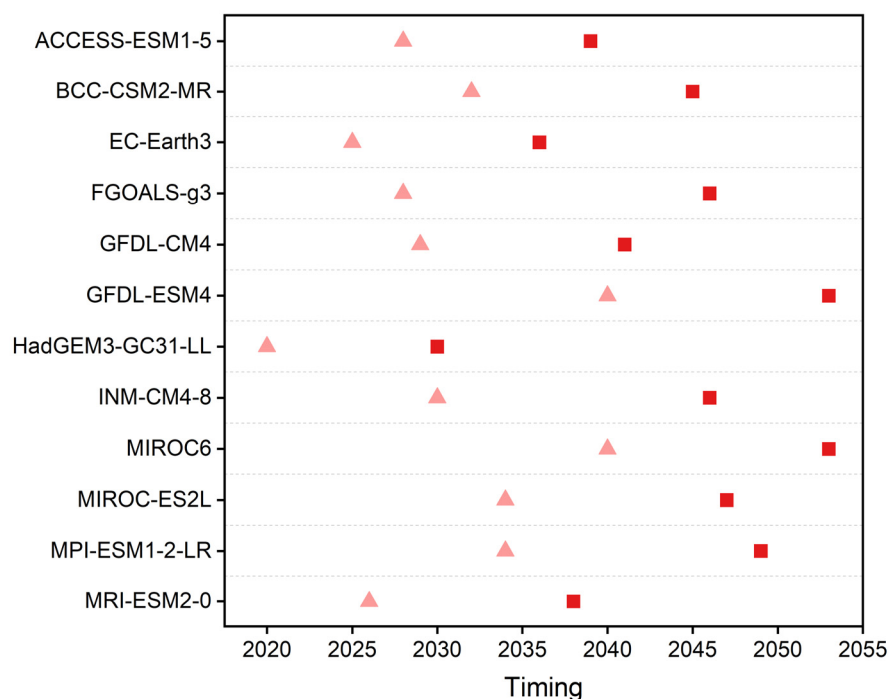


Figure 2. Timing to reach 1.5 °C (pink triangles) and 2 °C (red squares) global warming targets under SSP5-8.5. The year denotes the central timing of a 20-year time window.

3. Results

3.1. Dependence between Yield and Growing Season Temperature

Figure 3 shows the Spearman's rho between the detrended T_{GS} and yield for each crop and province. For rice, temperature and yield were significantly negatively correlated in Sichuan province ($\rho = -0.52$, $p < 0.05$), while they were significantly positively correlated in Heilongjiang ($\rho = 0.51$, $p < 0.05$) and Jiangsu ($\rho = 0.45$, $p < 0.05$) provinces as well as Guangxi Zhuang Autonomous Region ($\rho = 0.42$, $p < 0.05$). For wheat, temperature and yield were negatively correlated in the northwestern and southwestern provinces, with the lowest correlation coefficient of -0.55 ($p < 0.05$) in Sichuan province, while positive correlations were observed in northern China and the Yangtze River Delta provinces. In contrast, for maize, temperature and yield were negatively correlated for all provinces except Heilongjiang and Henan, with the lowest correlation coefficient of -0.48 ($p < 0.05$) in Liaoning province. The correlations between T_{GS} and yield are consistent with those in previous studies [27,40,42,43,60–63]. These results indicated that the dependence between yield and T_{GS} varied with crop and region. Overall, a negative correlation between yield and T_{GS} was observed in about half of the rice- and wheat-producing provinces and in the vast majority of the maize-producing provinces.

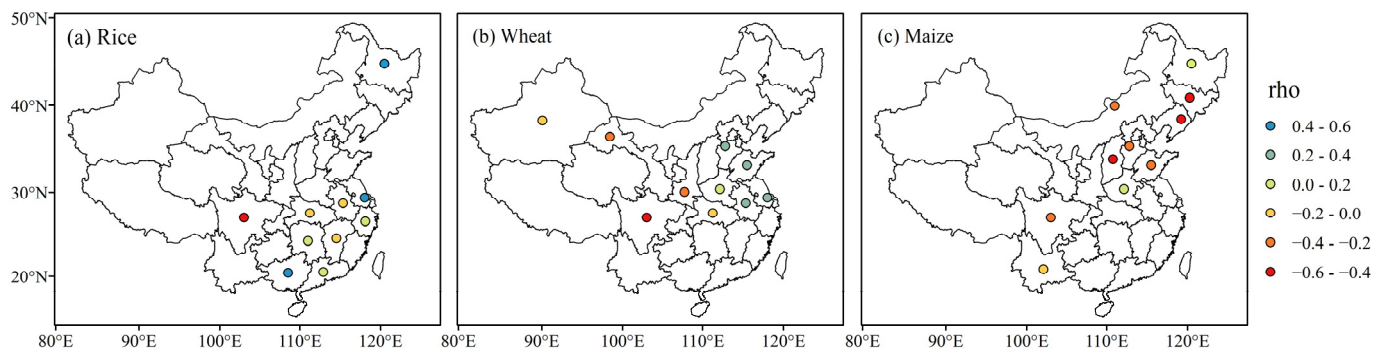


Figure 3. Spearman’s rank correlation coefficient (ρ) between the detrended yield and temperature.

Five copulas were fitted to the detrended T_{GS} and yield data, and then the optimal copula for each crop and province was selected according to AIC, as shown in Table 4. It can be seen that Archimedean copulas were more suitable for describing the joint distributions between T_{GS} and yield in most rice-producing provinces. For wheat-producing provinces, the optimal copulas were equally divided between elliptical and Archimedean copulas, while for maize-producing provinces, elliptical copulas dominated. Overall, there was a tail dependence between ΔT_{GS} and $\Delta Yield$ for more than 1/3 of the major producing provinces, indicating a higher probability of the simultaneous occurrence of extremes in temperature and yield.

Table 4. Optimal copula for each crop and province during the reference period (1995–2014).

| Province | Rice Copula | AIC | Province | Wheat Copula | AIC | Province | Maize Copula | AIC |
|----------|-------------|---------|----------|--------------|---------|----------|--------------|---------|
| HLJ | Gumbel | −129.48 | HB2 | Gaussian | −138.18 | HB2 | Gaussian | −124.70 |
| JS | Clayton | −140.28 | JS | Gumbel | −129.99 | SX2 | Gaussian | −123.97 |
| ZJ | Clayton | −125.73 | AH | Gumbel | −129.60 | NM | Gaussian | −139.33 |
| AH | Frank | −122.31 | SD | Frank | −133.21 | LN | Gaussian | −128.61 |
| JX | Frank | −132.39 | HN2 | Gumbel | −140.42 | JL | t | −127.13 |
| HB | Gaussian | −138.04 | HB | t | −129.41 | HLJ | Gaussian | −130.76 |
| HN | Clayton | −127.42 | SC | Gaussian | −126.49 | SD | Gaussian | −130.69 |
| GD | Gumbel | −130.47 | SX | Gaussian | −137.39 | HN2 | Clayton | −141.53 |
| GX | Gaussian | −138.24 | GS | Gaussian | −127.69 | SC | Gaussian | −129.09 |
| SC | Gaussian | −129.33 | XJ | Frank | −134.41 | YN | Gaussian | −140.45 |

For visualization, a typical province was chosen for each crop to illustrate the dependence characteristics between ΔT_{GS} and $\Delta Yield$. They are Heilongjiang province (rice), Sichuan province (wheat), and Hebei province (maize), which belong to the cold-temperate and temperate continental monsoon climate, subtropical monsoon climate, and temperate continental monsoon climate zones, respectively, indicating that they are under different heat conditions. Figure 4 compares the estimated $\Delta Yield$ distribution with the observed $\Delta Yield$ under different ΔT_{GS} during the reference period. Specifically, Heilongjiang province showed an upper tail dependence based on Gumbel copula, reflecting a greater probability of higher $\Delta Yield$ with higher ΔT_{GS} (Figure 4a). Taking wheat in Sichuan and maize in Hebei as examples, the joint distribution of ΔT_{GS} and $\Delta Yield$ based on Gaussian copula exhibited a symmetric dependence structure but with tail independence (Figure 4b,c). As seen, most of the $\Delta Yield$ fell in the high-density area of the PDF in all panels, indicating that the estimated distributions were reliable for describing the dependence between temperature and yield.

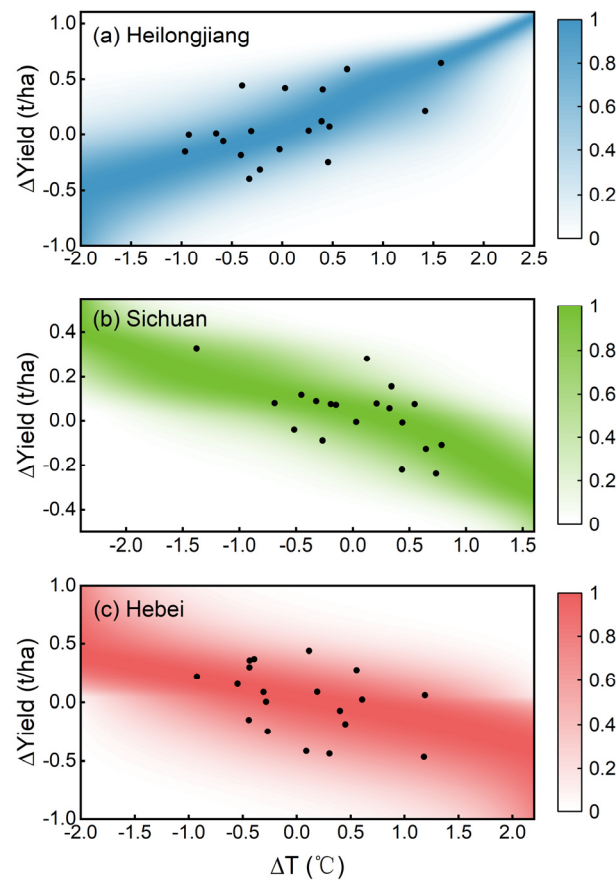


Figure 4. Joint distribution (normalized between 0 to 1) between detrended temperature (ΔT_{GS}) and yield ($\Delta Yield$) during the reference period for (a) Heilongjiang province (rice), (b) Sichuan province (wheat), and (c) Hebei province (maize), respectively. The colored pixels on the z-axis in each panel represent the probability density function (PDF) at a given ΔT_{GS} - $\Delta Yield$ pair, with 1 denoting the highest density and 0 denoting the lowest density. The black dots show the location of the observed $\Delta Yield$ at different ΔT_{GS} .

3.2. Conditional Probability of Yield Reduction under Different Warming Conditions

Based on the joint distribution of ΔT_{GS} and $\Delta Yield$, the conditional probabilities of yield variation under different warming conditions (herein $\Delta T_{GS} = 0.5^\circ\text{C}$, 1°C , 1.5°C , and 2°C) were estimated to reveal the sensitivity of yield to warming. As shown in Figure 5a, the conditional probability distribution of $\Delta Yield$ for rice in Heilongjiang province became more left-skewed with enhanced warming, indicating that yield was more likely to increase, or in other words, less likely to decrease, with warmer temperatures. By contrast, the conditional probability distribution of $\Delta Yield$ for wheat in Sichuan province and maize in Hebei province became more right-skewed as warming intensified (Figure 5b,c), suggesting a greater likelihood of yield reduction with warmer temperatures. These results indicated that the probability distribution of yield had different skewness and kurtosis under different warming conditions and varied with crop and province.

Based on the conditional PDF of yield for each crop and province, we estimated the conditional probability of yield reduction (i.e., $\Delta Yield < 0$) under different warming conditions by calculating the area under the PDF curve within the interval $(-\infty, 0]$. According to the correlation between yield and temperature (Figure 3), we divided the producing provinces of each crop into two parts, one with a negative temperature-yield correlation and the other with a positive temperature-yield correlation. The negative/positive temperature-yield correlation reflected the potential benefit/threat of warming on yield. Hence, provinces with a negative/positive correlation between temperature and yield were referred to as vulnerable/non-vulnerable provinces thereafter.

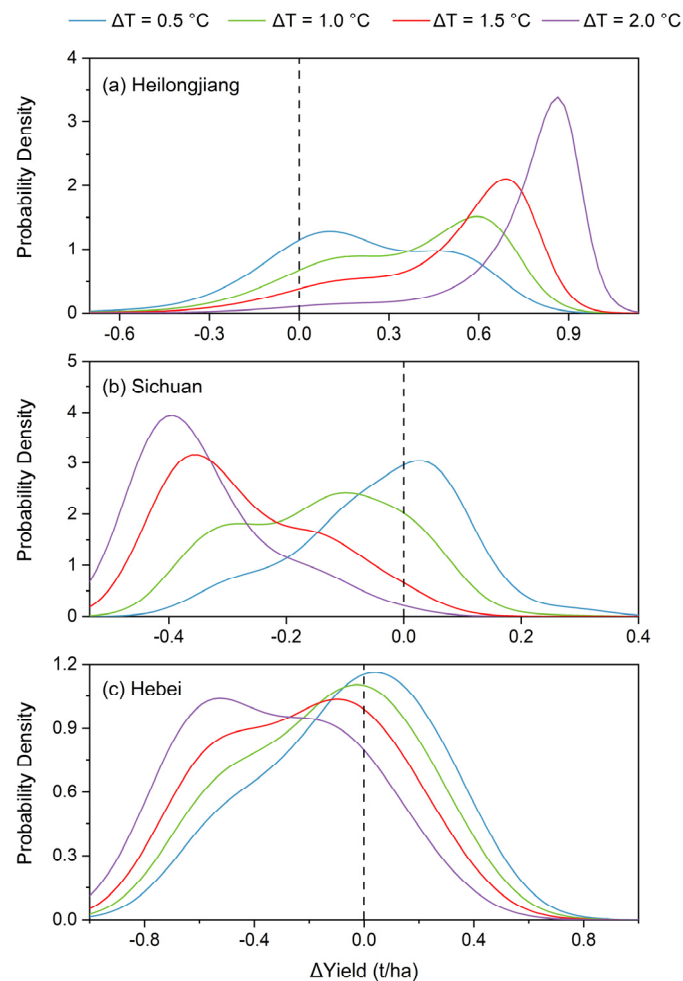


Figure 5. Conditional probability distribution of yield variation (Δ Yield) given four warming conditions ($\Delta T_{GS} = 0.5, 1, 1.5,$ and $2\text{ }^{\circ}\text{C}$) for (a) Heilongjiang province (rice), (b) Sichuan province (wheat), and (c) Hebei province (maize), respectively.

Figure 6 shows the overall probability of yield reduction for each crop under the four warming conditions. Overall, the yield reduction probability under warming for all three crops was higher in the vulnerable provinces than in the non-vulnerable provinces, with maize having a greater probability of yield reduction than rice and wheat. It should be noted that the difference in the probability of yield reduction for maize was smaller between vulnerable and non-vulnerable provinces than for rice and wheat (Figure 6c). This suggested that maize was at greater risk of warming-driven yield reduction than rice and wheat. Specifically, the upward gradient in the probability of maize yield reduction was greater in the vulnerable provinces than the downward gradient in the non-vulnerable provinces, indicating that the sensitivity of maize yield to warming was higher in the vulnerable provinces.

3.3. Future Global Warming and its Effect on Yield Reduction

The bias-corrected and downscaled temperature data were validated in the reference period by randomly selecting grid points within China. As shown in Figure 7, the multi-model ensemble mean of temperature presented a good agreement with the observed temperature ($R^2 = 0.976, p < 0.001$), indicating that the corrected simulation data could reproduce the temperature variation and therefore were suitable for future warming prediction. The future T_{GS} variations for each crop and province were then calculated at $1.5\text{ }^{\circ}\text{C}$ and $2\text{ }^{\circ}\text{C}$ global warming under SSP5-8.5 compared to the reference period. Overall, the magnitude of variation in T_{GS} varies with crop and is ranked under both global warming conditions:

maize > wheat > rice (Figure 8). Notably, the difference in T_{GS} variation between the 1.5 °C and 2 °C global warming will exceed 0.5 °C, indicating that the increasing gradient in T_{GS} between the two warming conditions is greater than that of GMST.

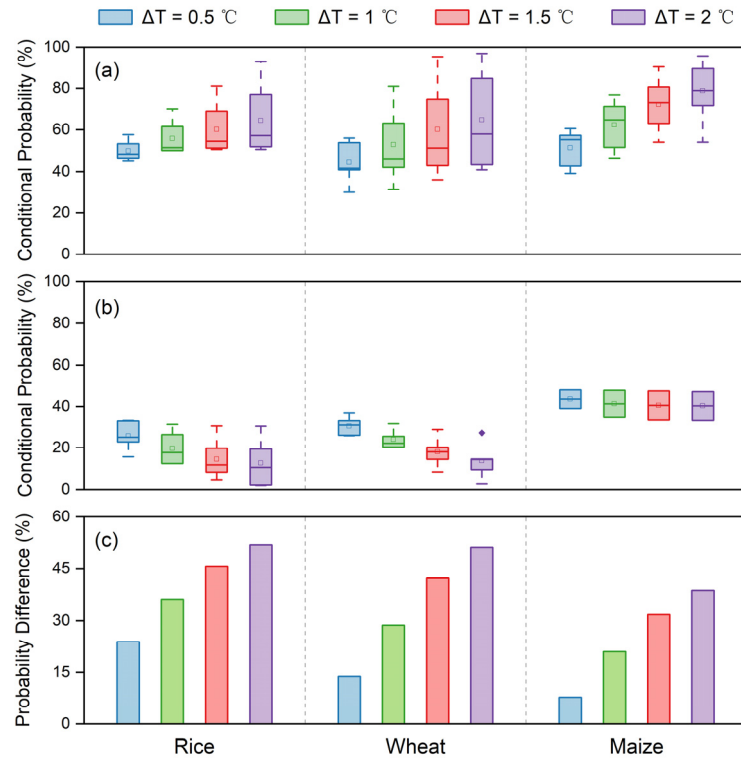


Figure 6. Conditional probability distribution of yield variation (Δ Yield) given four warming conditions ($\Delta T_{GS} = 0.5, 1, 1.5,$ and 2 °C) for provinces where yield and temperature were (a) negatively correlated and (b) positively correlated, respectively. The mean difference of conditional probability between (a,b) is shown in (c).

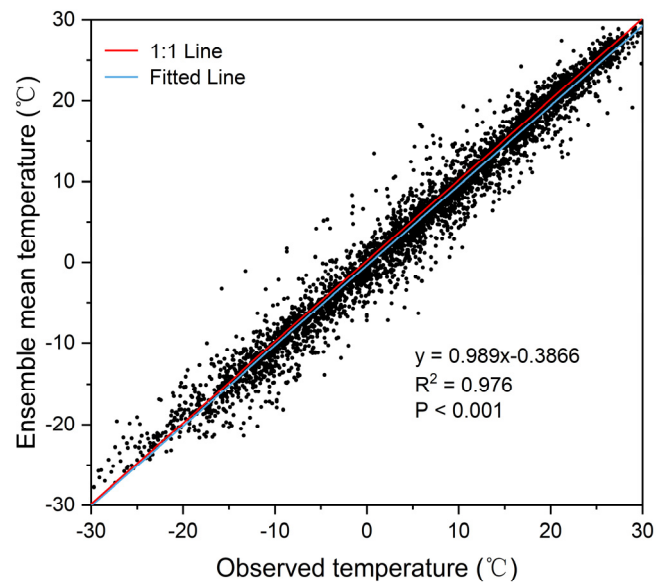


Figure 7. Validation of the ensemble mean temperature of the 12 CMIP6 models against the observed temperature. Each black dot represents a randomly selected grid point within China.

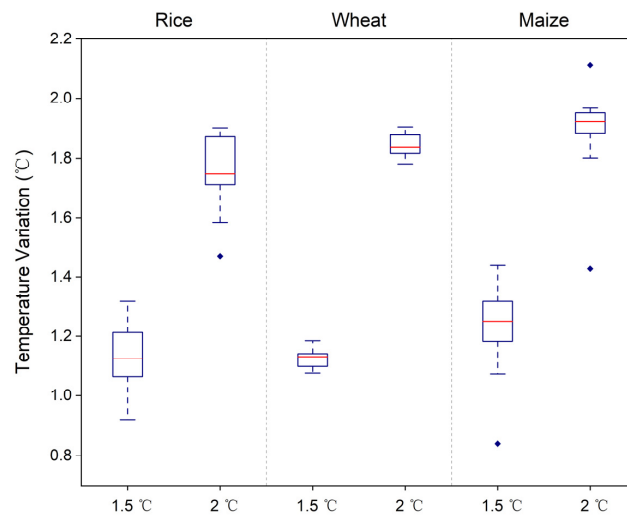


Figure 8. Growing season temperature variations in main crop-producing provinces at 1.5 °C and 2 °C global warming under SSP5-8.5 compared to the reference period (1995–2014).

Figure 9 shows the conditional probability of yield reduction ($\Delta\text{Yield} < 0$) for each crop and province estimated from the ensemble mean T_{GS} variation (ΔT_{GS}) at 1.5 °C and 2 °C global warming under SSP5-8.5. At the 1.5 °C global warming, the yield reduction probability will be 11–71%, 18–84%, and 34–87% among the main producing provinces for rice, wheat, and maize, respectively (Figure 9a–c). Overall, the spatial pattern of the yield reduction probability is consistent for both warming conditions. The most vulnerable crop-provinces cases under warming are rice in Sichuan province, wheat in the Sichuan and Gansu provinces, and maize in Shandong, Liaoning, Jilin, Nei Mongol, Shanxi, and Hebei provinces, in line with the spatial pattern of the temperature-yield correlation (Figure 3). These provinces should be prioritized for developing climate adaptation strategies.

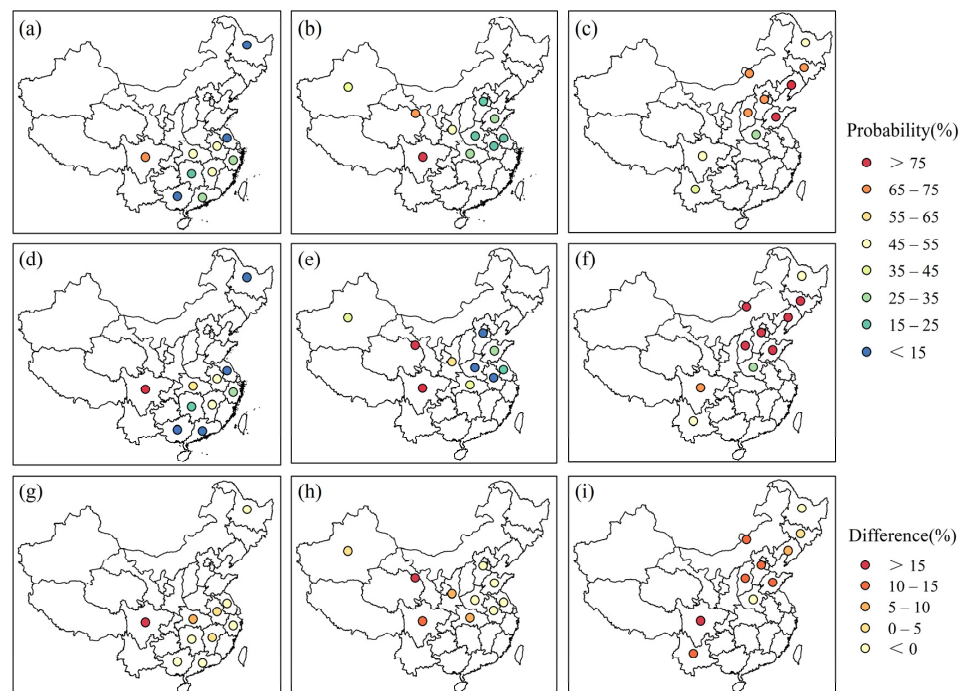


Figure 9. Probability of yield reduction for rice (first column, a,d,g), wheat (second column, b,e,h), and maize (third column, c,f,i) at 1.5 °C (top row, a–c) and 2 °C (middle row, d–f) global warming under SSP5-8.5. The difference in the probability of yield reduction between 1.5 °C and 2 °C global warming is shown in the bottom row.

When additional global warming of 0.5 °C occurs (i.e., the 2 °C global warming condition), the probability of yield reduction will increase by 2–17%, 1–16%, and 3–17% for rice, wheat, and maize, respectively, in the vulnerable provinces, while declining to different degrees in the non-vulnerable provinces (Figure 9g–i). This suggests that the additional warming would pose a greater risk of yield reduction in the vulnerable provinces, while mitigating the yield reduction risk in non-vulnerable provinces. For instance, the risk of rice yield reduction will increase by 17% in Sichuan province, while it will decrease by 8% in Heilongjiang province.

4. Discussion

4.1. Crop Yield Response to Warming Conditions

The dependence characteristics between the detrended T_{GS} (ΔT_{GS}) and yield (ΔYield) showed an apparent spatial heterogeneity (Figure 3 and Table 4), indicating that yield response to temperature varied with crop and region. For example, rice yield and temperature were negatively correlated in Sichuan province, while they were positively correlated in Heilongjiang and Jiangsu provinces; the temperature was positively correlated with wheat yield and negatively correlated with maize yield in Shandong province. These results were broadly consistent with previous studies conducted at different scales over China, though to different degrees [21,39,40,64–66]. Generally, the warming effect on yield is twofold and closely related to the optimum temperature for crop growth [67]. On the one hand, warming can inhibit crop growth, especially during the heading-flowering stage, which shortens the growth period and thus reduces biomass accumulation [53,66,68,69]. For example, Sichuan province is relatively abundant in heat, so yields for all three crops were under warming stress (Figure 3). On the other hand, for some heat-deficient regions (e.g., Heilongjiang province), warming can converge the temperature to the optimum temperature for crop growth, thus enhancing photosynthesis and increasing biomass [21,64,66,70]. In addition, yield response to temperature is also influenced by other external factors, such as water supply [71]. For example, a study on U.S. maize showed that precipitation substantially altered the magnitude of temperature-driven yield changes [8]. A global-scale study indicated that the compound dry-hot condition had a greater impact on maize yields than the individual hot condition [72].

Based on the dependence between yield and temperature, we divided all provinces into two parts, those threatened by warming (vulnerable provinces) and those benefiting from it (non-vulnerable provinces). This study focused on the risk of yield reduction in vulnerable provinces. Figure 9g–i shows that an additional 0.5 °C of global warming will increase the yield reduction risk in vulnerable provinces by 2–17%, 1–16%, and 3–17% for rice, wheat, and maize, respectively. Since provinces vulnerable to warming account for about half of the major rice- and wheat-producing provinces and most maize-producing provinces (Figure 3), the risk of yield reduction in these provinces would threaten China's agricultural productivity and total crop production. Hence, it is necessary to limit global warming to 1.5 °C to avoid the adverse effects of global warming on crop yields and thus protect food supplies.

Overall, the copula-based models proved to be an effective tool for investigating the temperature-yield relationship in different cropping systems and regions of China. Unlike the deterministic estimates of previous studies, the copula model can provide yield distribution given any temperature condition and further offer probabilistic estimates of yield loss risk. This can help farmers and stakeholders manage agricultural operations to meet the complex challenges of future climate change [73]. Previous studies have shown that copula can be flexibly applied to explore the relationship between yield and other yield-related climatic factors (e.g., precipitation and drought) [11,23,73]. Furthermore, by extending the bivariate model to a trivariate model, it is possible to estimate the yield loss risk under a combination of two climatic conditions (e.g., temperature and precipitation/drought) [72,74].

4.2. Uncertainties and Limitations

There are some uncertainties and limitations in this study. First, the dependence between temperature and yield was related to the chosen reference period and the growing period of

a given crop, which may influence the trend and magnitude of yield changes under different temperature conditions. Second, this study only considered the effect of temperature on yield, but the yield is influenced by the combined effects of multiple climatic factors, such as drought, CO₂ concentration, and extreme events [5,13,27,66]. For instance, with and without considering the effect of CO₂ fertilization, yield reduction was projected to be less than 15% and 14% for maize and wheat in most areas of China under the 2 °C global warming condition [66]. Third, this study assumed that the temperature-yield relationship obtained in the reference period remained unchanged in the future. However, adaptive measures and technological improvements (e.g., changes in planting time and cultivars, irrigation, and fertilization) can partly offset the adverse effect of climate change on yield and thus alter the temperature-yield relationship [24,65,75,76]. Finally, uncertainties may derive from the model structure and parameters, the spatial and temporal scales, and other factors [27,29,76]. As a result, the probability of yield reduction under global warming may be underestimated or overestimated. However, despite these uncertainties, this study provided a reasonable estimate of the yield loss risk in China's major crops and producing provinces under global warming. Future work can be extended to the county scale and incorporate other influencing factors into the copula model to obtain more accurate estimates of yield loss risk under global change.

5. Conclusions

This study used a probabilistic approach based on bivariate copulas to explore the dependence between yield and growing season temperature in major producing provinces of China for three staple crops, i.e., rice, wheat, and maize. The probability of yield reduction for each crop and province under 1.5 °C and 2 °C global warming conditions was then estimated based on the joint distribution of yield and temperature obtained from the optimal copulas. The main conclusions are as follows:

- (1) The dependence between yield and growing season temperature varied with crop and region. Overall, Archimedean/elliptical copulas provided the best fits of joint distribution between T_{GS} and yield in most rice-/maize-producing provinces. There were four rice-producing provinces, five wheat-producing provinces, and eight maize-producing provinces vulnerable to warming pressures. The most vulnerable crop-province cases were rice in Sichuan province, wheat in the Sichuan and Gansu provinces, and maize in the Shandong, Liaoning, Jilin, Nei Mongol, Shanxi, and Hebei provinces.
- (2) The yield reduction probability under warming was overall higher in vulnerable provinces than in non-vulnerable provinces, with maize having a greater yield reduction risk than rice and wheat. The sensitivity of maize yield to warming gradient was higher in vulnerable provinces than in non-vulnerable provinces.
- (3) From 1.5 °C to 2 °C global warming, an additional 0.5 °C of warming could increase the risk of yield reduction in vulnerable provinces by 2–17%, 1–16%, and 3–17% for rice, wheat, and maize, respectively.

Author Contributions: Formal analysis, methodology, conceptualization, and writing—original draft, F.W.; investigation, data curation, C.Z.; methodology, writing—review and editing, L.Z. All authors have read and agreed to the published version of the manuscript.

Funding: This research was funded by the National Natural Science Foundation of China (U22A20555), the Strategic Priority Research Program of the Chinese Academy of Sciences (Grant No. XDA23040304), and the Project funded by China Postdoctoral Science Foundation (2021M703178).

Data Availability Statement: The datasets used or analyzed during the current study are available on reasonable request.

Conflicts of Interest: The authors declare that they have no conflict of interest.

References

1. IPCC. Summary for Policymakers. In *Climate Change 2021: The Physical Science Basis*. In *Climate Change 2021: The Physical Science Basis. Contribution of Working Group I to the Sixth Assessment Report of the Intergovernmental Panel on Climate Change*; IPCC: Cambridge, UK; New York, NY, USA, 2021; pp. 3–32.
2. Asseng, S.; Ewert, F.; Martre, P.; Rötter, R.P.; Lobell, D.B.; Cammarano, D.; Kimball, B.A.; Ottman, M.J.; Wall, G.W.; White, J.W.; et al. Rising temperatures reduce global wheat production. *Nat. Clim. Change* **2014**, *5*, 143–147. [[CrossRef](#)]
3. Baulcombe, D.; Crute, I.; Davies, B.; Dunwell, J.; Gale, M.; Jones, J.; Pretty, J.; Sutherland, W.; Toulmin, C. *Reaping the Benefits: Science and the Sustainable Intensification of Global Agriculture*; Royal Society: London, UK, 2009; p. 72.
4. Gourdji, S.M.; Sibley, A.M.; Lobell, D.B. Global crop exposure to critical high temperatures in the reproductive period: Historical trends and future projections. *Environ. Res. Lett.* **2013**, *8*, 024041. [[CrossRef](#)]
5. Lobell, D.B.; Schlenker, W.; Costa-Roberts, J. Climate Trends and Global Crop Production Since 1980. *Science* **2011**, *333*, 616–620. [[CrossRef](#)] [[PubMed](#)]
6. Tilman, D.; Balzer, C.; Hill, J.; Befort, B.L. Global food demand and the sustainable intensification of agriculture. *Proc. Natl. Acad. Sci. USA* **2011**, *108*, 20260–20264. [[CrossRef](#)]
7. IBRD. *World Development Report 2008: Agriculture for Development*; World Bank: Washington, DC, USA, 2007.
8. Leng, G. Uncertainty in Assessing Temperature Impact on U.S. Maize Yield Under Global Warming: The Role of Compounding Precipitation Effect. *J. Geophys. Res. Atmos.* **2019**, *124*, 6238–6246. [[CrossRef](#)]
9. Lobell, D.B.; Cahill, K.N.; Field, C.B. Historical effects of temperature and precipitation on California crop yields. *Clim. Change* **2007**, *81*, 187–203. [[CrossRef](#)]
10. Hatfield, J.L.; Prueger, J.H. Temperature extremes: Effect on plant growth and development. *Weather Clim. Extrem.* **2015**, *10*, 4–10. [[CrossRef](#)]
11. Madadgar, S.; AghaKouchak, A.; Farahmand, A.; Davis, S.J. Probabilistic estimates of drought impacts on agricultural production. *Geophys. Res. Lett.* **2017**, *44*, 7799–7807. [[CrossRef](#)]
12. Matiu, M.; Ankerst, D.P.; Menzel, A. Interactions between temperature and drought in global and regional crop yield variability during 1961–2014. *PLoS ONE* **2017**, *12*, e0178339. [[CrossRef](#)]
13. Peña-Gallardo, M.; Vicente-Serrano, S.M.; Quiring, S.; Svoboda, M.; Hannaford, J.; Tomas-Burguera, M.; Martín-Hernández, N.; Domínguez-Castro, F.; El Kenawy, A. Response of crop yield to different time-scales of drought in the United States: Spatio-temporal patterns and climatic and environmental drivers. *Agric. For. Meteorol.* **2019**, *264*, 40–55. [[CrossRef](#)]
14. Zhao, C.; Liu, B.; Piao, S.; Wang, X.; Lobell, D.B.; Huang, Y.; Huang, M.; Yao, Y.; Bassu, S.; Ciais, P.; et al. Temperature increase reduces global yields of major crops in four independent estimates. *Proc. Natl. Acad. Sci. USA* **2017**, *114*, 9326–9331. [[CrossRef](#)] [[PubMed](#)]
15. Feng, S.; Hao, Z.; Wu, X.; Zhang, X.; Hao, F. A multi-index evaluation of changes in compound dry and hot events of global maize areas. *J. Hydrol.* **2021**, *602*, 126728. [[CrossRef](#)]
16. Ottman, M.J.; Kimball, B.A.; White, J.W.; Wall, G.W. Wheat Growth Response to Increased Temperature from Varied Planting Dates and Supplemental Infrared Heating. *Agron. J.* **2012**, *104*, 7–16. [[CrossRef](#)]
17. Wheeler, T.R.; Craufurd, P.Q.; Ellis, R.H.; Porter, J.R.; Vara Prasad, P.V. Temperature variability and the yield of annual crops. *Agric. Ecosyst. Environ.* **2000**, *82*, 159–167. [[CrossRef](#)]
18. He, Y.; Hu, X.; Xu, W.; Fang, J.; Shi, P. Increased probability and severity of compound dry and hot growing seasons over world's major croplands. *Sci. Total Environ.* **2022**, *824*, 153885. [[CrossRef](#)] [[PubMed](#)]
19. Deryng, D.; Sacks, W.J.; Barford, C.C.; Ramankutty, N. Simulating the effects of climate and agricultural management practices on global crop yield. *Glob. Biogeochem. Cycles* **2011**, *25*, GB2006. [[CrossRef](#)]
20. O'Connell, E. Towards Adaptation of Water Resource Systems to Climatic and Socio-Economic Change. *Water Resour. Manag.* **2017**, *31*, 2965–2984. [[CrossRef](#)]
21. Zhang, H.; Tao, F.; Xiao, D.; Shi, W.; Liu, F.; Zhang, S.; Liu, Y.; Wang, M.; Bai, H. Contributions of climate, varieties, and agronomic management to rice yield change in the past three decades in China. *Front. Earth Sci.* **2015**, *10*, 315–327. [[CrossRef](#)]
22. Chen, H.; Liang, Z.; Liu, Y.; Jiang, Q.; Xie, S. Effects of drought and flood on crop production in China across 1949–2015: Spatial heterogeneity analysis with Bayesian hierarchical modeling. *Nat. Hazards* **2018**, *92*, 525–541. [[CrossRef](#)]
23. Leng, G. Keeping global warming within 1.5 degrees C reduces future risk of yield loss in the United States: A probabilistic modeling approach. *Sci. Total Environ.* **2018**, *644*, 52–59. [[CrossRef](#)]
24. Olesen, J.E.; Trnka, M.; Kersebaum, K.C.; Skjelvåg, A.O.; Seguin, B.; Peltonen-Sainio, P.; Rossi, F.; Kozyra, J.; Micale, F. Impacts and adaptation of European crop production systems to climate change. *Eur. J. Agron.* **2011**, *34*, 96–112. [[CrossRef](#)]
25. Ray, D.K.; Gerber, J.S.; MacDonald, G.K.; West, P.C. Climate variation explains a third of global crop yield variability. *Nat. Commun.* **2015**, *6*, 5989. [[CrossRef](#)] [[PubMed](#)]
26. Tao, F.; Yokozawa, M.; Liu, J.; Zhang, Z. Climate–crop yield relationships at provincial scales in China and the impacts of recent climate trends. *Clim. Res.* **2008**, *38*, 83–94. [[CrossRef](#)]
27. Zhang, Z.; Song, X.; Tao, F.; Zhang, S.; Shi, W. Climate trends and crop production in China at county scale, 1980 to 2008. *Theor. Appl. Climatol.* **2015**, *123*, 291–302. [[CrossRef](#)]
28. Tao, F.; Hayashi, Y.; Zhang, Z.; Sakamoto, T.; Yokozawa, M. Global warming, rice production, and water use in China: Developing a probabilistic assessment. *Agric. For. Meteorol.* **2008**, *148*, 94–110. [[CrossRef](#)]

29. Tao, F.; Rotter, R.P.; Palosuo, T.; Gregorio Hernandez Diaz-Ambrona, C.; Minguuez, M.I.; Semenov, M.A.; Kersebaum, K.C.; Nendel, C.; Specka, X.; Hoffmann, H.; et al. Contribution of crop model structure, parameters and climate projections to uncertainty in climate change impact assessments. *Glob. Chang. Biol.* **2018**, *24*, 1291–1307. [[CrossRef](#)]
30. Ferrise, R.; Moriondo, M.; Bindi, M. Probabilistic assessments of climate change impacts on durum wheat in the Mediterranean region. *Nat. Hazards Earth Syst. Sci.* **2011**, *11*, 1293–1302. [[CrossRef](#)]
31. Iizumi, T.; Yokozawa, M.; Nishimori, M. Probabilistic evaluation of climate change impacts on paddy rice productivity in Japan. *Clim. Change* **2010**, *107*, 391–415. [[CrossRef](#)]
32. Moradkhani, H.; Madadgar, S. A Bayesian Framework for Probabilistic Seasonal Drought Forecasting. *J. Hydrometeorol.* **2013**, *14*, 1685–1705. [[CrossRef](#)]
33. Nelson, R.B. *An Introduction to Copulas*, 2nd ed.; Springer: New York, NY, USA, 2006; pp. 1–248.
34. UNFCCC. *Adoption of the Paris Agreement. Proposal by the President*; United Nations: Paris, France, 2015.
35. Barry, S.; Cai, Y. Climate change and agriculture in China. *Glob. Environ. Change* **1996**, *6*, 205–214.
36. Laborte, A.G.; Gutierrez, M.A.; Balanza, J.G.; Saito, K.; Zwart, S.J.; Boschetti, M.; Murty, M.V.R.; Villano, L.; Aunario, J.K.; Reinke, R.; et al. RiceAtlas, a spatial database of global rice calendars and production. *Sci. Data* **2017**, *4*, 170074. [[CrossRef](#)]
37. You, L.; Rosegrant, M.W.; Wood, S.; Sun, D. Impact of growing season temperature on wheat productivity in China. *Agric. For. Meteorol.* **2009**, *149*, 1009–1014. [[CrossRef](#)]
38. *National Agricultural Atlas of China*; China Cartographic Publishing House: Beijing, China, 1989.
39. Tao, F.; Zhang, S.; Zhang, Z.; Rötter, R.P. Temporal and spatial changes of maize yield potentials and yield gaps in the past three decades in China. *Agric. Ecosyst. Environ.* **2015**, *208*, 12–20. [[CrossRef](#)]
40. Chen, C.; Zhou, G.S.; Pang, Y.M. Impacts of climate change on maize and winter wheat yields in China from 1961 to 2010 based on provincial data. *J. Agric. Sci.* **2014**, *153*, 825–836. [[CrossRef](#)]
41. Tao, F.; Zhang, Z.; Shi, W.; Liu, Y.; Xiao, D.; Zhang, S.; Zhu, Z.; Wang, M.; Liu, F. Single rice growth period was prolonged by cultivars shifts, but yield was damaged by climate change during 1981–2009 in China, and late rice was just opposite. *Glob. Chang. Biol.* **2013**, *19*, 3200–3209. [[CrossRef](#)]
42. Tao, F.; Zhang, Z.; Xiao, D.; Zhang, S.; Rötter, R.P.; Shi, W.; Liu, Y.; Wang, M.; Liu, F.; Zhang, H. Responses of wheat growth and yield to climate change in different climate zones of China, 1981–2009. *Agric. For. Meteorol.* **2014**, *189–190*, 91–104. [[CrossRef](#)]
43. Liu, S.-L.; Pu, C.; Ren, Y.-X.; Zhao, X.-L.; Zhao, X.; Chen, F.; Xiao, X.-P.; Zhang, H.-L. Yield variation of double-rice in response to climate change in Southern China. *Eur. J. Agron.* **2016**, *81*, 161–168. [[CrossRef](#)]
44. Wu, J.; Gao, X. A gridded daily observation dataset over China region and comparison with the other datasets. *Chin. J. Geophys.* **2013**, *56*, 1102–1111.
45. Zhou, B.; Xu, Y.; Wu, J.; Dong, S.; Shi, Y. Changes in temperature and precipitation extreme indices over China: Analysis of a high-resolution grid dataset. *Int. J. Climatol.* **2016**, *36*, 1051–1066. [[CrossRef](#)]
46. Wu, J.; Gao, X.; Giorgi, F.; Chen, D. Changes of effective temperature and cold/hot days in late decades over China based on a high resolution gridded observation dataset. *Int. J. Climatol.* **2017**, *37*, 788–800. [[CrossRef](#)]
47. Zhang, X.; Hua, L.; Jiang, D. Assessment of CMIP6 model performance for temperature and precipitation in Xinjiang, China. *Atmos. Ocean. Sci. Lett.* **2022**, *15*, 100128. [[CrossRef](#)]
48. Su, B.; Huang, J.; Fischer, T.; Wang, Y.; Kundzewicz, Z.W.; Zhai, J.; Sun, H.; Wang, A.; Zeng, X.; Wang, G.; et al. Drought losses in China might double between the 1.5 degrees C and 2.0 degrees C warming. *Proc. Natl. Acad. Sci. USA* **2018**, *115*, 10600–10605. [[CrossRef](#)]
49. Wang, J.; Song, C.; Reager, J.T.; Yao, F.; Famiglietti, J.S.; Sheng, Y.; MacDonald, G.M.; Brun, F.; Schmied, H.M.; Marston, R.A.; et al. Recent global decline in endorheic basin water storages. *Nat. Geosci.* **2018**, *11*, 926–932. [[CrossRef](#)] [[PubMed](#)]
50. Wood, A.W. Long-range experimental hydrologic forecasting for the eastern United States. *J. Geophys. Res.* **2002**, *107*, 4429. [[CrossRef](#)]
51. Leng, G.; Huang, M.; Voisin, N.; Zhang, X.; Asrar, G.R.; Leung, L.R. Emergence of new hydrologic regimes of surface water resources in the conterminous United States under future warming. *Environ. Res. Lett.* **2016**, *11*, 114003. [[CrossRef](#)]
52. Xu, L.; Wang, A. Application of the Bias Correction and Spatial Downscaling Algorithm on the Temperature Extremes from CMIP5 Multimodel Ensembles in China. *Earth Space Sci.* **2019**, *6*, 2508–2524. [[CrossRef](#)]
53. Tao, F.; Zhang, Z.; Zhang, S.; Zhu, Z.; Shi, W. Response of crop yields to climate trends since 1980 in China. *Clim. Res.* **2012**, *54*, 233–247. [[CrossRef](#)]
54. Feng, S.; Hao, Z. Quantifying likelihoods of extreme occurrences causing maize yield reduction at the global scale. *Sci. Total Environ.* **2020**, *704*, 135250. [[CrossRef](#)]
55. Joe, H. *Multivariate Models and Dependence Concepts*, 1st ed.; Chapman & Hall: London, UK; New York, NY, USA, 1997.
56. Sklar, A. Fonctions de répartition à n dimensions et leurs marges. *Publ. Inst. Statist. Univ. Paris* **1959**, *8*, 229–231.
57. Jiang, J.; Huang, S.; Huang, Q.; Ren, K.; Leng, G.; Wang, H.; Guo, Y.; Bai, Q. Copula-based non-stationarity identification of watershed water and energy dependency structure and possible driving forces. *Atmos. Res.* **2022**, *279*, 106396. [[CrossRef](#)]
58. Mazdiyasi, O.; AghaKouchak, A.; Davis, S.J.; Madadgar, S.; Mehran, A.; Ragno, E.; Sadegh, M.; Sengupta, A.; Ghosh, S.; Dhanya, C.T.; et al. Increasing probability of mortality during Indian heat waves. *Sci. Adv.* **2017**, *3*, e1700066. [[CrossRef](#)]
59. Sadegh, M.; Ragno, E.; AghaKouchak, A. Multivariate Copula Analysis Toolbox (MvCAT): Describing dependence and underlying uncertainty using a Bayesian framework. *Water Resour. Res.* **2017**, *53*, 5166–5183. [[CrossRef](#)]

60. Che, X.; Li, H.; Zhang, C.; Guo, D.; Shen, H. Impacts of climate change on corn yield in Jilin province since 1980s. *Res. Soil Water Conserv.* **2021**, *28*, 230–234+241. [[CrossRef](#)]
61. Zuo, H.; Lou, Y.; Li, Z.; Shi, Y.; Zheng, Z.; Wang, Y. Analysis and prediction of major climate factors controlling rice yield in typical climate regions of China. *J. Nat. Disasters* **2018**, *27*, 114–125.
62. Ye, H.; Shi, X.; Di, D.; Hua, S.; Xu, Z. Ensemble simulation of impacts of climate change on rice production in Zhejiang Province. *Acta Agric. Zhejiangensis* **2016**, *28*, 1183–1192.
63. Yu, H.; Lu, W.; Cao, S.; Chen, C. Impacts of temperature and precipitation resources change on rice-wheat production in recent 20 years in Jiangsu Province. *Resour. Environ. Yangtze Basin* **2015**, *24*, 1876–1883.
64. Bai, H.; Tao, F.; Xiao, D.; Liu, F.; Zhang, H. Attribution of yield change for rice-wheat rotation system in China to climate change, cultivars and agronomic management in the past three decades. *Clim. Change* **2015**, *135*, 539–553. [[CrossRef](#)]
65. Chen, C.; Zhou, G.-s.; Zhou, L. Impacts of Climate Change on Rice Yield in China From 1961 to 2010 Based on Provincial Data. *J. Integr. Agric.* **2014**, *13*, 1555–1564. [[CrossRef](#)]
66. Chen, Y.; Zhang, Z.; Tao, F. Impacts of climate change and climate extremes on major crops productivity in China at a global warming of 1.5 and 2.0 °C. *Earth Syst. Dyn.* **2018**, *9*, 543–562. [[CrossRef](#)]
67. Porter, J.R.; Gawith, M. Temperatures and the growth and development of wheat: A review. *Eur. J. Agron.* **1999**, *10*, 23–36. [[CrossRef](#)]
68. Peng, S.; Tang, Q.; Zou, Y. Current Status and Challenges of Rice Production in China. *Plant Prod. Sci.* **2015**, *12*, 3–8. [[CrossRef](#)]
69. Zhang, Z.; Wang, P.; Chen, Y.; Song, X.; Wei, X.; Shi, P. Global warming over 1960–2009 did increase heat stress and reduce cold stress in the major rice-planting areas across China. *Eur. J. Agron.* **2014**, *59*, 49–56. [[CrossRef](#)]
70. Zhang, Z.; Liu, X.; Wang, P.; Shuai, J.; Chen, Y.; Song, X.; Tao, F. The heat deficit index depicts the responses of rice yield to climate change in the northeastern three provinces of China. *Reg. Environ. Change* **2013**, *14*, 27–38. [[CrossRef](#)]
71. Proctor, J.; Rigden, A.; Chan, D.; Huybers, P. More accurate specification of water supply shows its importance for global crop production. *Nat. Food* **2022**, *3*, 753–763. [[CrossRef](#)]
72. Feng, S.; Hao, Z.; Zhang, X.; Hao, F. Probabilistic evaluation of the impact of compound dry-hot events on global maize yields. *Sci. Total Environ.* **2019**, *689*, 1228–1234. [[CrossRef](#)] [[PubMed](#)]
73. Ribeiro, A.F.S.; Russo, A.; Gouveia, C.M.; Páscoa, P.; Pires, C.A.L. Probabilistic modelling of the dependence between rainfed crops and drought hazard. *Nat. Hazards Earth Syst. Sci.* **2019**, *19*, 2795–2809. [[CrossRef](#)]
74. Feng, S.; Hao, Z.; Zhang, X.; Hao, F. Changes in climate-crop yield relationships affect risks of crop yield reduction. *Agric. For. Meteorol.* **2021**, *304–305*, 108401. [[CrossRef](#)]
75. Challinor, A.J.; Watson, J.; Lobell, D.B.; Howden, S.M.; Smith, D.R.; Chhetri, N. A meta-analysis of crop yield under climate change and adaptation. *Nat. Clim. Change* **2014**, *4*, 287–291. [[CrossRef](#)]
76. Knutti, R.; Sedláček, J. Robustness and uncertainties in the new CMIP5 climate model projections. *Nat. Clim. Change* **2012**, *3*, 369–373. [[CrossRef](#)]

Disclaimer/Publisher’s Note: The statements, opinions and data contained in all publications are solely those of the individual author(s) and contributor(s) and not of MDPI and/or the editor(s). MDPI and/or the editor(s) disclaim responsibility for any injury to people or property resulting from any ideas, methods, instructions or products referred to in the content.